MHD Stability Studies in Reversed Shear Plasmas in TFTR

J. Manickam, E. Fredrickson, Z. Chang, M. Okabayashi,
M. Bell, W. Park, G. Schmidt, M. C. Zarnstorff,
and the TFTR group
Princeton Plasma Physics Laboratory, Princeton NJ USA
and
F. Levinton and S. Batha
Fusion Physics and Technology, Torrance CA USA
and
T. C. Hender, C. G. Gimblett, R. J. Hastie
UKAEA/EURATOM Fusion Association, Culham, Abingdon, UK
and
M. Phillips, and M. H. Hughes
Northrop-Grumman, Plainsboro NJ USA

F1-CN-64/A5-2

MHD Stability Studies in Reversed Shear Plasmas in TFTR

Abstract

MHD phenomena in reversed shear plasmas in TFTR are described during each of the three phases of the evolution of these discharges: the current ramp, high power neutral beam heating and after the beam power has been reduced. Theoretical analysis of discharges which disrupted in the high-β phase indicates that the β -limit is set by the ideal $n = 1$ infernal/kink mode. The mode structure of the disruption precursor reconstructed from the electron temperature data compares favorably with the predicted displacement vector from the ideal MHD model. In contrast, disruptions during the early and late phases are due to resistive instabilities, double tearing modes coupled to high-m edge modes. The resistive interchange mode, predicted to be unstable in reversed shear plasmas, is not seen in the experiment. Neo-classical tearing mode theory is shown to describe the non-disruptive MHD phenomena. A nonlinear resistive MHD simulation reproduces off-axis sawtooth-like crashes during the post-beam phase. The dependence of the β -limit on the pressure peakedness and $q_{\min}$ is discussed, showing a path to stable higher-β regimes.

Tokamak plasmas having safety-factor profiles with shear reversal in the core are attractive for several reasons: a) improved stability to high-n ballooning modes[1], where n is the toroidal mode number, b) the potential for aligning the self-generated bootstrap currents with a stable current distribution[2], c) improved microstability which may result in improved confinement[2] and d) stabilization of neo-classical (bootstrap driven) instabilities in the reverse shear region[3].

This regime of reversed shear (RS) plasmas has been the subject of intense interest on many large tokamaks including the Tokamak Fusion Test Reactor, TFTR. In TFTR RS plasmas a spontaneous transition to improved confinement is often observed; this plasma regime is referred to as the Enhanced Reversed Shear (ERS) regime. This report will focus on the MHD properties of RS and ERS plasmas in TFTR.

1. Plasma Evolution

RS plasmas are produced by heating the plasma during the current rise phase of the discharge to slow the penetration of the current to the core. The resulting off-axis maximum of the current density results in a reversed shear q-profile.

However it should be noted that the profile is not static and continues to evolve slowly as the current diffuses and as the pressure-driven bootstrap current is generated. The q-profile is mainly characterised by $q_{edge}, q_{axis}, q_{min}$ and r_{qmin}, the location of the q_{min}-surface. For the reasons outlined above, it is only possible to maintain $q_{\rm edge}$ at a constant value, $q_{\rm min}$ and $r_{\rm q-min}$ steadily decrease during the discharge. In most of the discharges $q_{\rm min}$ dropped to about 2 at the end of the heating phase. This aspect of RS operation plays a significant role in the context of MHD stability and will be discussed later. The pressure profile in RS plasmas is similar to those in supershots and is fairly peaked with a peakedness defined as PPF $\equiv \ p_0/\langle p\rangle$ typically 4. Here p_0 represents the pressure on axis and $<>$ represents a volume average. In ERS plasmas the improved confinement causes the pressure profile to peak even more and results in PPF ≥ 6.

The RS and ERS discharges are limited in the achievable β by rapidly growing MHD instabilities, where $\beta \equiv 2\mu_0 < p > /B^2$, B is the vacuum toroidal field. It is often possible to prevent the disruptions by reducing the beam power after a prescribed period of high-power heating, $i.e.$ by limiting the rise in β . In spite of this, some of the discharges disrupt after the beam power is reduced. Some even disrupt at very low β well after the beams have been turned off. A useful measure of the stored energy is the normalized β, $\beta_N \equiv \beta/(\frac{I}{aB})$ where I is the current in Mega Amps, a, the plasma minor radius in meters, and B is measured in Tesla. A better indicator of the fusion power achievable is $\beta^* \equiv 2\mu_0 < p^2 >^{\frac{1}{2}} /B^2$. Typically $\beta^* > \beta$ and β^* /β increases as PPF increases. In TFTR ERS discharges for PPF $\sim$ 4, $\beta^*/\beta \sim 1.5$ and for PPF $\sim$ 7, $\beta^*/\beta \sim 2$. An analogous expression to β_N, for the normalized β^* is $\beta^*_N \equiv \beta^*/(\frac{I}{aB})$. In TFTR, most of the experiments were conducted in plasmas with a current of either 1.6 MA or 2.2 MA. The highest β_N achieved at 1.6 MA was β_N $\sim$2 and at 2.2 MA it was β_N $\sim$ 1.7. The corresponding values of β^*_N are 3.8 and 2.9 respectively.

2. Observed MHD

The discharge has different forms of MHD activity in the three distinct beam heating phases. The early phase, referred to as the $prelude$, when low beam power is used to freeze the $q-$profile, the $high\ power$ phase when the plasma β increases, and the post-beam phase, referred to as the $postlude$, when the beam power is reduced or even turned off. There is no significant difference in the MHD activity in RS and ERS plasmas, except that ERS plasmas reach higher values of β and may experience β -limiting disruptions.

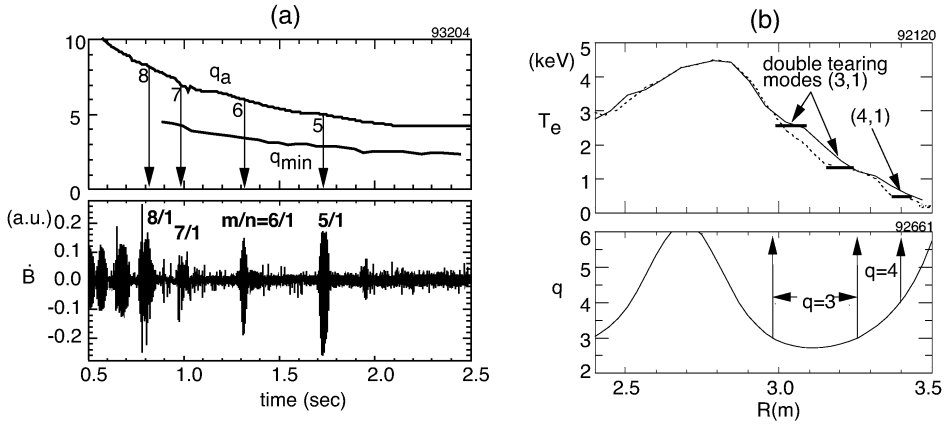

Figure 1: MHD activity during the prelude phase includes: **a)** Bursts associated with $q_{\rm edge}$ or $q_{\rm min}$ passing through integer values, and **b)** The flat spots in the temperature profiles indicate the presence of tearing modes localized near the rational surfaces.

The principal diagnostics for the MHD are the external Mirnov loops and the internal electron cyclotron emission, ECE, measurements of the electron temperature. Depending on the mode characteristics, internal and/or external, MHD events are observed on one or both of the diagnostics. The q profile is measured by the Motional Stark Effect, MSE, diagnostic.

In the $prelude$ the MHD activity is seen on both Mirnov and ECE and is correlated with either $q_{\rm min}$ or $q_{\rm edge}$ passing through integer values. Figure 1a shows the evolution of q_{edge}, $q_{\rm min}$ and the signals from the Mirnov data. A clear correlation of the MHD activity with $q_{\rm edge}$ is observed. Figure 1b shows the electron temperature profile reconstructed from the ECE grating polychromator and the q profile from the MSE. A double tearing mode is observed localized near the two q =3 surfaces. The toroidal mode number, $n = 1$, and the poloidal mode number, m, is inferred to be 3. There is also a tearing mode at the q =4 surface. In some instances when the double tearing mode is coupled to the higher m edge modes, the plasma may disrupt.

During the main heating phase, there are two forms of MHD activity. There

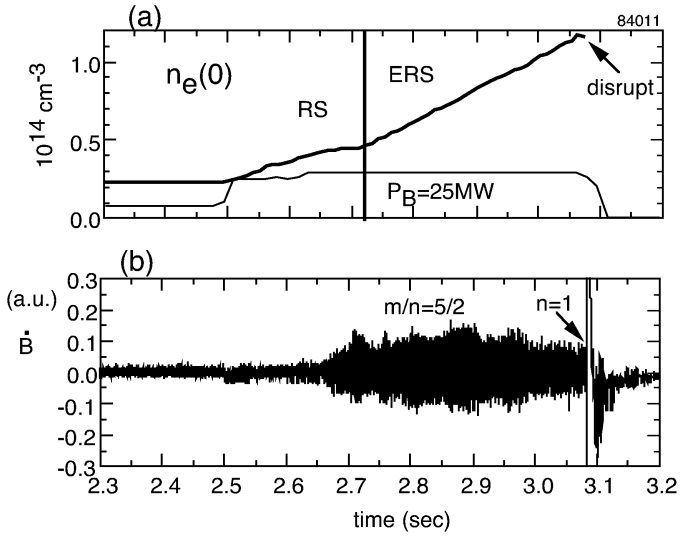

Figure 2: **a)**MHD during the high power heating phase does not affect the rise in stored energy. **b)**Disruptions with an $n = 1$ precursor are observed at high β .

is continuous MHD activity as observed on the Mirnov loop signal. The ECE diagnosticis shows that this is usually located at and beyond the $r_{\mathrm{q-min}}$ radius.As seen in Fig. 2 it has no apparent effect on the evolution of the discharge, and generally corresponds to a toroidal mode number, $n = 2$, and is determined to be co-rotating with the plasma. In some discharges a concurrent $n = 1$ or $n = 3$ mode is seen. As the stored energy rises an $n = 1$ mode may grow rapidly, also shown in Fig. 2, leading to a disruption. The mode is located in the vicinity of the $q_{\min}$ surface. In some disruptions a ballooning mode located in the positive shear region is observed, superposed on the $n = 1$ mode. This is similar to the observation in supershot plasmas[4]. Disruptions determine the β-limit in these plasmas.

In the post-beam phase of ERS plasmas there is often a periodic drop in the core temperature in a manner similar to a sawtooth. However as $q_{\min}$ remains above unity, and the central temperature remains high, this is a different form of sawtooth-like collapse, see Fig. 3.

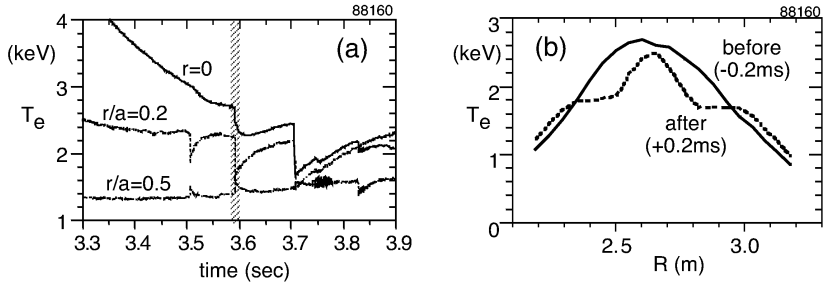

Figure 3: Electron temperature profile shows an off-axis flattening of the T_e profile as a result of a periodic sawtooth-like collapse, **a)** three cords showing, an off-axis heat pulse, r/a =0.2, 0.5, while the central cord, $r/a = 0$ is relativly unchanged, **b)** $T_e(R)$ profiles 0.2 $ms.$ before and after the crash at 3.6 seconds, see the shaded region in a). In some events the reconnection extends to the core, as seen at 3.7 seconds.

3. Analysis

The stability analysis of RS and ERS discharges has focussed mainly on the high power and postlude phases. It starts with a reconstruction of the plasma equilibrium profiles. The q -profile is determined by the Motional Stark Effect diagnostic, when it is available, or the data from a similar shot is used. It should be noted that the MSE diagnostic is not available during the high power phase. The evolution of the current profile in the high power phase is based on resistive diffusion, using the TRANSP code. The pressure profile is also determined by TRANSP based on the measured T_e, T_i, n_e profiles an other measured plasma parameters. To account for the uncertainity of the reconstruction, and to determine the sensitivity to the details of the profiles, equilibria with possible profile modifications are also considered. These equilibria are examined using a number of MHD stability codes as well as analytic methods.

Several high-β discharges which disrupted were examined and the predicted stability limit compared to the experimental value at the disruption. Table I shows the comparison of the β limit as well as some key plasma parameters at

the time of disruption. The disruptive β limit is identified to be caused by an ideal $n = 1$ instability, an infernal/kink mode[5]. It is driven primarily by the pressure gradient in the low shear region, and consequently is sensitive to the location of rational surfaces. In the high current discharges it also has a large edge component. The high-n ballooning modes are stable across the plasma.

	1.6 MA			2.2 MA		
Shot No.	85693	85694	84011	91788	93260	93517
Expt. β_N	1.3	1.7	1.7	1.2	1.3	1.7
Theory $\beta_N^{Crit.}$	1.5	1.7	1.7	1.3	1.3	1.8
Disrupted	NO	YES	YES	YES	YES	YES
$q_{\min}$	2.2	2.0	2.0	1.8	2.0	1.9
$p_o/\langle p \rangle$	4.5	6.5	7.5	8.0	6.4	4.2

Table 1: Comparison of the theoretically predicted $\beta_N^{Crit.}$ with the maximum β_N observed in the experiment prior to the disruption. One non-disruptive case is included for comparison.

The predicted infernal/kink mode structure can be compared with a mode structure reconstructed from the ECE data. The contours of constant electron temperature are monitored and their displacement is used to determine the radial displacement of the flux surfaces. Figure 4 shows such a comparison for discharge number 93260. The ECE diagnostic is less reliable near the plasma boundary, however supplemental information is available by extrapolating the Mirnov signal back to the plasma edge assuming that $\xi_r \propto (r - r_{edge})^m$, where m is the poloidal mode number corresponding to nq_{edge}. The agreement between this reconstruction and the theoretical prediction from the PEST code is remarkable. A similar favorable comparison was made for discharge 84011 at 1.6 MA. This implies that the theoretical β -limit from ideal theory is a good guide to the stability properties of RS and ERS plasmas. Parametric dependence of the β -limits is discussed later in this report.

During the high power phase there is continuous MHD activity, which is inferred to be resistive in nature because the growth-times are on the resistive time scale and mode rotation is close to the plasma rotation. Theoretical analysis indicates that the resistive interchange criterion[6] is violated when the shear, q', is negative and the pressure gradient, p', is sufficiently large. In the experiment these conditions are often satisfied. However the mode is not seen at the ratio-

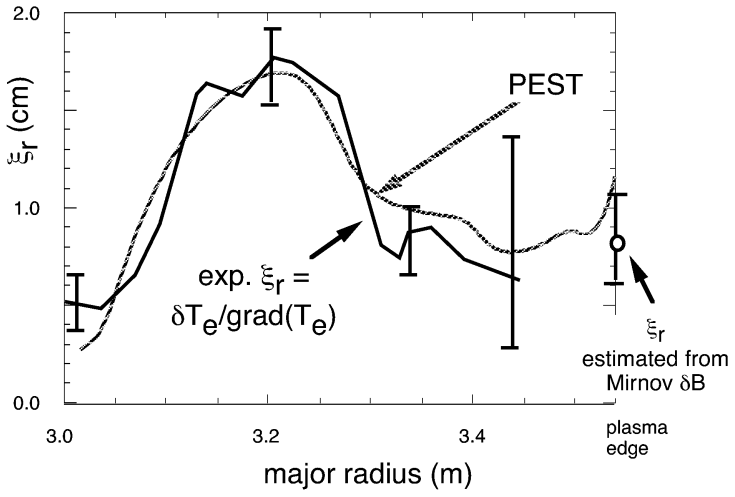

Figure 4: Comparison of the predicted radial displacement vector along the outer mid-plane for a plasma at the β -limit with the reconstruction using the temperature data for a disruption precursor in a 2.2 MA discharge. Note that the maximum amplitude of the PEST ξ_r was scaled to match the maximum of the experimental ξ_r.

nal surface in the negative shear region, rather the mode is seen at the rational surface in the positive shear region where the interchange mode is inherently stable, since $q' > 0$. Neo-classical tearing modes are a better candidate for this activity. In fact neo-classical theory indicates that the tearing and interchange modes are stabilized in the negative shear region and tearing modes are destabilized in regions with positive shear. Comparison of the evolution of the island-width inferred from the Mirnov data agrees well with the predictions of analytic theory[3].

The off-axis sawtooth observed in the post-beam phase is simulated with the non-linear resistive MHD code, MH3D[7]. A double tearing mode is shown to cause a magnetic reconnection and a thermal heat pulse. As the simulation evolves a hot island moves out and a cold island moves inwards. A comparison of the the T_e profiles from the experiment and the simulation is shown in Fig. 5.

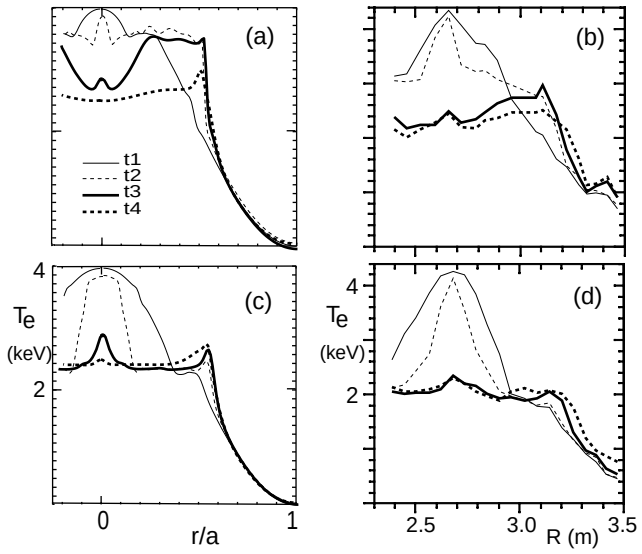

Figure 5: Comparison of MH3D simulation (on the left) and experimental observation from 2 ECE systems (on the right) of a 2/1 sawtooth core reconnection. Four phases can be distinguished: (1) Early growth phase (t_1). (2) Double-tearing reconnection phase (t_2). (3) Central temperature callapse phase (t_3). (4) Final temperature equalization phase (t_4). The basic feature is the inner hot island moving out [(a) and (b)], and the outer cold island moving in [(c) and (d)].

4. Parameter dependence

The preceding analysis suggests that the β limit observed in TFTR discharges is governed by stability to the ideal $n = 1$ instability. It is largely an internal mode and is sensitive to various plasma parameters, including; $\beta, \beta^*, PPF, q_{min}, r_{qmin}, q'_{edge}$. A general study of these dependencies was reported in Ref. [8]. Details of a specific study using profiles from the experiment as a starting point are presented here. Figure 6a shows the dependence of the critical β_N and β_N^* for instability on the peakedness of the pressure profile, $p_o/\langle p\rangle$. After a modest increase there is a clear decline in the critical β_N as $p_o/\langle p\rangle$ increases, an optimal value is $p_o/\langle p\rangle$ = 3.5. It is interesting to note that while β_N declines as $p_o/\langle p\rangle$ is increased, β_N^* rises and is essentially independent of $p_o/\langle p\rangle$. This bodes well for the use of ERS type plasmas in an advanced tokamak. Figure 6b show the dependence on $q_{\min}$ at fixed $p_o/\langle p\rangle$. The variation in the critical values of β_N

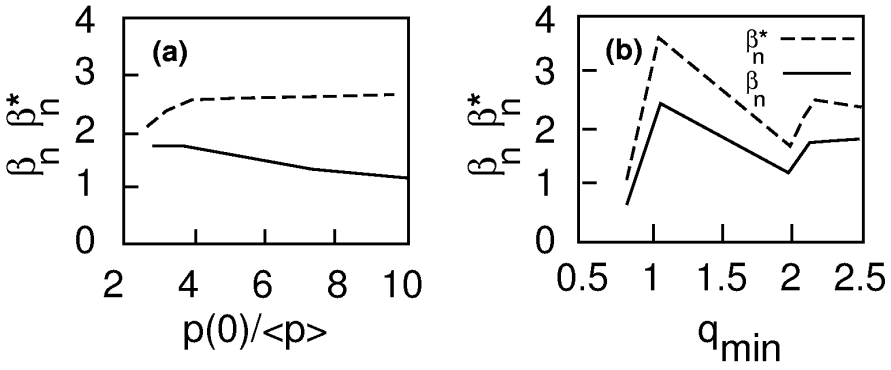

Figure 6: **a)** For large values of $p_o/\langle p\rangle$, the critical β_N^* is independent of the pressure peakedness. **b)** There is a sudden drop in β_N and β_N^* when $q_{\min}$ is an integer.

and β_N^* show a strong dependence on $q_{\min}$. The optimal value is $q_{min} \sim 1.2$. An analytic theory of the beta limit when the minimum in the q -profile lies just below a rational value has been developed [9]. In this limit the eigenfunction is adequately represented by three poloidal harmonics and a relatively low β-limit with $\beta_{crit} \propto \epsilon^{8/5}$ is found, ϵ is the inverse aspect ratio. The instability is described as a double kink.

5. Summary

This report describes the main experimental observations in RS and ERS plasmas in TFTR. Disruptions set a β-limit in these discharges. Detailed modelling of the experiment during the high power phase shows that the ideal $n = 1$, infernal/kink instability is responsible for the observed disruptions. The mode structure of the disruption precursor is shown to compare favorably with the prediction of ideal MHD theory. The role of resistive MHD in the RS and ERS plasmas is more complex. Resistive interchange modes, predicted to be unstable in the negative shear region of the plasma are not observed. Tearing

modes are seen to play a role during the prelude and postlude phases. The resistive MHD observed during the high power phase is apparently benign and has been identified as neo-classical tearing modes. The absence of the better known resistive modes coupled with the strong agreement with ideal MHD theory, confirms that the TFTR plasmas are deep in the collisionless regime, a regime of particular relevance to tokamak reactors.

Analytic and numerical methods have been used to uncover the underlying physics of the instability. The peakedness of the pressure profile plays a key role in two ways. It is responsible for directly driving the instability, and is the source of the bootstrap current which modifies the q -profile leading to greater instability. $q_{\min}$ is shown to have a critical role. Specifically when nq_{min} is approximately an integer the probability of driving an instability increases. Careful tailoring of the q -profile can achieve improved stability limits.

This paper has concentrated largely on the performance limiting MHD issues. Several MHD stability issues remain to be addressed. In particular, analysis of the MHD activity in the prelude phase and some of the disruptions in the postlude phase remains to be studied.

Acknowledgement: This work was supported by the US Department of Energy under contract No. DE-AC02-76-CHO-3073. UKAEA authors were supported jointly by the UK Department of Trade and Industry and EURATOM.

References

[1] Greene, J. M., Chance, M. S., Nuc. Fusion **21** (1981) 453.

[2] Kessel, C., et al., Phys. Rev. Lett. **72** (1994) 1212.

[3] Chang, Z., et al., Phys. Rev. Lett. **74** (1995) 4663-4666.

[4] Park, W., et al., Phys. Rev. Lett. **75** (1995) 1763-1766 .

[5] Manickam, J., et. al., Nuc. Fusion **27** (1987) 1461-1472.

[6] Glassser, A., Greene, J. M., Johnson, J. L., Phys. Fluids **18** (1975) 875.

[7] Chang, Z. et al., Phys. Rev. Lett. to be published.

[8] Phillips, M. et al., Phys. Plasmas **3** (1996) 1673.

[9] Gimblett C., et al., Phys. Plasmas **3** (1996) 3369-3374.